

Numerical Study of Heat Conduction Enhancement of a Latent Heat Thermal Energy Storage (LHTES) Device Using Finned Tubes.

George Maliaris*, Sofia Kavafaki, Charalampos Pelagiadis and Nikolaos Kokkinos

Additive Manufacturing Laboratory, Dept. of Chemistry, School of Science, International Hellenic University, 65 404, Ag. Loukas, Kavala, Greece.

Received 21 November 2022; Accepted 8 April 2023

Abstract

The objective of this paper is to examine the thermal performance of a LHTES system comprised of a single tube, by means of a Computational Fluid Dynamics (CFD) computer code. Two different types of fins, straight and annular, were considered to enhance the heat conduction between the tube and the RT42 Phase Change Material (PCM). The dimensions of the fins were elected so that the total area of the fins to be almost equal, in both configurations. The RT42 PCM is a paraffin wax with medium to high thermal energy storage and chemically inert. Whereas possible, temperature dependent thermal properties, provided by the producer, used for the definition of the material model. Between the finless tube and the one with straight fins, the melting time reduction was approximately 56.7% and between the finless and the annular tube, the PCM melt time was reduced by 61.5%. Heat conduction was the driving heat transfer mechanism during the first seconds of the PCM melting process. On the other hand, natural convection was the lead heat transfer method as the liquid PCM was able to move due to density and temperature differences. The investigation of the liquid PCM travel revealed that in the finless model and the one with the straight fins the PCM movement was parallel to the axial direction whereas in the model with the annular fins the velocity of the PCM was parallel to the radial direction.

Keywords: CFD, PCM, LHTES

1. Introduction

The level of modern consumption contributes significantly to the major ecological and societal challenges of our times: resource depletion, climate change, biodiversity reduction, air and soil pollution [1]. Europe has adopted the European Green Deal with 9 policy areas in order to overcome these challenges. One of the key principles for the clean energy transition is the prioritization of energy efficiency. Thermal Energy Storage (TES) technologies can play a significant role for improving energy efficiency, since they provide means to balance energy supply and demand in time. Among the various energy storage technologies, phase change thermal storage, or Latent Heat Energy Storage (LHTES), has received extensive attention due to its advantages including large latent heat and almost constant temperature during charging or discharging stages. One of the significant drawbacks of these systems is the low thermal conductivity of the PCMs involved. To overcome this issue many researchers proposed the enhancement of the heat transfer through the increase of the available total heat conduction surface using metallic fins [2, 3]. Although experimental setups have been proven valuable in providing information for understanding the physical mechanisms of heat transfer in LHTES systems, numerical methods are capable of providing deeper insight. Up to now, in many research works numerical methods have been implemented to study heat transfer in LHTES systems, but with restrictions regarding the dimensions and the boundary conditions of the developed numerical models [4, 5].

Woodfield et al. [6] studied a phase change problem for non-isothermal incompressible viscous flows. The underlying

continuum was modelled as a viscous Newtonian fluid where the change of phase was either encoded in the viscosity itself, or in the Brinkman–Boussinesq approximation where the solidification process influences the drag directly. In [7] the authors simulated the melting and solidification process of silicone rubber/paraffin@SiO₂ shape-stabilized phase change material (SR/Pn@SiO₂). The effects of heating conditions and the content of phase change microcapsules on the heat transfer process of SR/Pn@SiO₂ were studied. An experimental system was developed to test the heat storage of SR/Pn@SiO₂ composites. Based on the thermal-physical and macroscopic geometrical properties of SR/Pa@SiO₂ composites, the volume-averaged method was selected to investigate their heat transfer characteristics and behavior. In work of Wang et al [8], numerical simulation for freezing of paraffin (RT28) and CuO nanoparticles were applied through a geometry containing radial fins. Three models for fins with same surface area were applied and container was full of Nanoparticle-Enhanced PCM (NEPCM). Unsteady modeling within two-dimensional container with involve of fins was simulated with finite volume approach. In governing equation, buoyancy term has been added and ANSYS FLUENT with incorporation of implicit approach were utilized for solving the equations. PRESTO algorithm was applied for correction of pressure and SIMPLE approach for linkage of velocity and pressure. Silica composite phase change materials (SiO₂-PCMs) were prepared by the sol-gel method, and SiO₂-PCMs with better performance was applied to an asphalt mixture. The finite element heat transfer model was established by measuring the boundary conditions, and the temperature adjustment effect was predicted and analyzed. The thermal performance of asphalt mixtures tests was simulated through the heat conduction finite element

*E-mail address: gmaliari@chem.ihu.gr

ISSN: 1791-2377 © 2023 School of Science, IHU. All rights reserved.

doi:10.25103/jestr.162.04

methods (FEM) in ABAQUS [9]. A series of paraffin-based ternary composite phase-change materials (PCMs) were prepared in work of Fang et al [10] by combining paraffin (PA) with expanded graphite (EG) and nano-copper (Cu) in a two-step method. The paraffin used had a melting temperature of 62-64°C. The thermal properties of the composite PCMs were studied by establishing an experimental test system and a simulation model. The solidification/melting model in the Fluent software was used for the simulation. The research work of Musaedi et al. [11] attempts to simulate the process of melting and solidification of paraffin phase change materials RT22, RT24, RT26 inside a multi-layer heat exchanger to store and release heat energy based on latent heat during phase transition. In this computer work, by examining the dimensions and temperature, the interactions of the heat transfer, buoyancy force and the viscosity have been evaluated. In [12] the authors studied the effects of PCM in periodic cellular structures fabricated by additive manufacturing for the purpose of being used as passive heat sinks. An experimental setup was used, as well as a simplified numerical simulation method. The material that was used for the periodic cellular structure was an aluminium alloy AISi10Mg, while the PCM materials that were impregnated in its structure were paraffin based, named RT42, RT55 and RT64HC. The impregnation was done via heating the PCM until a liquid state was achieved and pouring it into the structure until volume saturation was achieved. ANSYS-FLUENT software was used for the numerical solution of the solid-liquid phase change problem by using the finite element method, deriving temperature-time plots and temperature maps. Wei Cui et al [13] investigated the effect of metal foam-fin hybrid structures and inclination angle on the phase change process of PCM. The PCM that was used was Paraffin 52-54 and the numerical simulation for the solidification and melting processes was conducted via the use of ANSYS-FLUENT software, which included finite volume method, SIMPLE and PRESTO methods.

Most of the works found in literature are focused on scaled down versions of the actual LHTES systems or on a small segment of the structure that is used to enhance heat transfer. Although most of them consider PCM melting, the velocity gradients are not explored and also it is not mentioned whether gravity is activated or not. Thus, heat transfer with natural convection is not investigated thoroughly.

2. Model Description

2.1. Physical Model

In the present work, a shell – and – tube heat exchanger, with two kinds of fins, straight and annular, and one without fins was modelled and presented in Fig. 1. It consists of a shell and a tube with PCM material filling their in between space. The total length of the tube is 150mm, the inside diameter 20mm and the wall has a thickness of 1mm. The length of the shell is 110mm with a wall thickness of 5mm. The outside diameter of the shell is approximately 60mm. The tube and the shell are concentric. The gravity vector is parallel to the tube's axis. Both parts are considered to be from stainless steel. The volume between the tube and the shell, which is filled with the PCM material, is equal to 18.96cm³.

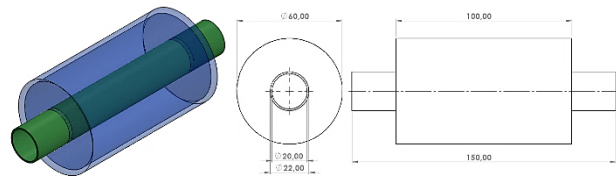


Fig. 1. Geometry and dimensions of the shell – and – tube heat exchanger without fins.

The PCM chosen for heat storage is RT42 from Rubitherm. It is a paraffin with high thermal energy storage capacity (165 kJ/kg), chemically inert with stable performance through the phase change cycles. Since it was of interest to describe the material thermal behavior as accurate as possible, density and viscosity are defined as a function of temperature. The fluid inside the tube is water. In the following figure 2, the thermal properties of RT42 are presented.

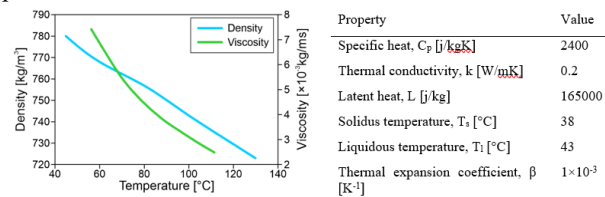


Fig. 2. Thermal properties of the PCM RT42.

One of the disadvantages of LHTES systems is the limited heat transfer coefficient of the organic phase change materials. That leads to very slow melting and solidification times, which is not acceptable in many applications. Among the proposed solutions, the enhancement of the heat transfer through the increase of the available total heat conduction surface using metallic fins attached on the tubes of a shell and tube exchanger, is the one that is commonly applied. As it is expected, and supported by the findings of other researchers [14, 15], as the heat conduction area increases, melting and solidification times decrease. Although it is possible to raise the total heat conduction area with a low surface to volume ratio geometry, the corresponding structures (e.g. aluminum foam) have a rather complicated geometry which in turn renders difficult the import and usage (especially the discretization and meshing with finite elements) in a simulation of the melting/ solidification process. Also, the manufacturing process of metallic foams with open cells is challenging and they are not cost effective with respect to their intended use. In this work, two types of fins with simplified geometries are considered, straight and annular ones and they are benchmarked against a simple tube without fins. Special care has been taken in order to keep the total surface area of the fins equal in both configurations for better comparison of the obtained results. In Fig. 3a the first configuration, which uses straight fins, is illustrated. The fin thickness is 1mm, total length 95mm, the diametral distance between two fins 53mm and the total number of fins attached on the tube is twelve. The annular fin type is used in the second case is presented in Fig. 3b. As with the straight fin, the thickness of the annular type is also 1mm. Additionally, the diameter of the fin is 52mm and the total number of fins attached on the tube is 10 with an axial distance of 7.80mm. The material of the tube and the fins is stainless steel with a density of 8030 kg/m³, specific heat 502 Jkg⁻¹K⁻¹ and thermal conductivity of 16.43 Wm⁻¹K⁻¹.

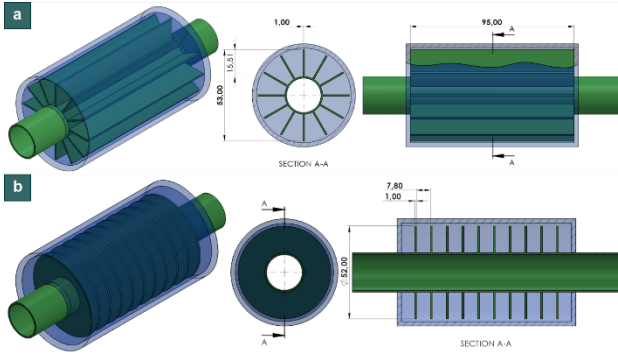


Fig. 3. The geometries and corresponding dimensions of the two configurations of the heat exchanger.

2.2. Computational Model

2.2.1. Governing Equations

The governing equations include continuity equation, momentum equation and energy equation.

Continuity equation:

$$\nabla \cdot \vec{u} = 0 \quad (1)$$

Momentum equation:

$$\rho_f \frac{\partial \vec{u}}{\partial t} + \rho_f (\vec{u} \cdot \nabla) \vec{u} = -\nabla P + \mu_f \nabla^2 \vec{u} + \rho_f \vec{g} \beta (T_f - T_m) + A \vec{u} \quad (2)$$

where ρ is the density, P is the pressure, μ is the dynamic viscosity, and β is the thermal expansion coefficient. Here, ∇ is the Laplace operator. The last term in equation (2) is an additional source for damping the velocity in the solid PCM [16].

$$A = \frac{c(1-f_l)^2}{s+f_l^3} \quad (3)$$

where C and S are the simulation coefficients that have been proposed [17] to be 1×10^5 and 1×10^{-3} , respectively. f_l represents the liquid fraction of PCM that varies depending on the temperature of the PCM. It is given by:

$$f_l = \begin{cases} 0 & T_f \leq T_{m1} \\ (T_f - T_{m1}) / (T_{m2} - T_{m1}) & T_{m1} \leq T_f \leq T_{m2} \\ 1 & T_f \geq T_{m2} \end{cases} \quad (4)$$

Energy equation:

The heat-transfer process of the PCM and the finned tube is complex, and includes conduction, phase-change, and convection heat transfer. Heat transfer in the PCM is described as:

$$\rho_f c_f \frac{\partial T_f}{\partial t} + \rho_f c_f \vec{u} \cdot \nabla T_f = \nabla \cdot (k_f \nabla T_f) - \rho_f \dot{L} \frac{\partial f_l}{\partial t} \quad (5)$$

Heat transfer in the solid material (tube, fins, shell) is defined as:

$$\rho_s c_{ps} \frac{\partial T_s}{\partial t} = \nabla \cdot (k_s \nabla T_s) \quad (6)$$

2.2.2. Model Assumptions

In order to numerically describe the transient heat transfer process and the phase change of the PCM, the following assumptions were proposed:

- The external surfaces of the shell and the tube are considered to be adiabatic.
- The liquid PCM is Newtonian and not compressible.
- Density variations were considered during PCM melting.
- There is no volume exchange between the liquid and solid states of the paraffin.
- Natural convection was considered during the melting of the paraffin.

2.2.3. Boundary Conditions

An initial temperature of 30°C was defined for all parts. The water flowing inside the tube had a velocity of 0.05m/s and temperature of 50°C for all configurations. A zero-heat flux condition was applied on the external adiabatic surfaces. Gravity vector aligned with the tube axis.

2.2.4. Numerical Conditions

A grid independence study was performed to keep solution parameters variation due to grid size within an acceptable range (lower than 3%). Fig. 4 presents the development of liquid fraction calculated with three different grid sizes, for the model with the annular fins. As it is depicted from the last figure, the numerical solution had an acceptable accuracy when the grid size was set equal to 0.2mm, which resulted to a total number of more than 100×10^6 mesh grids.

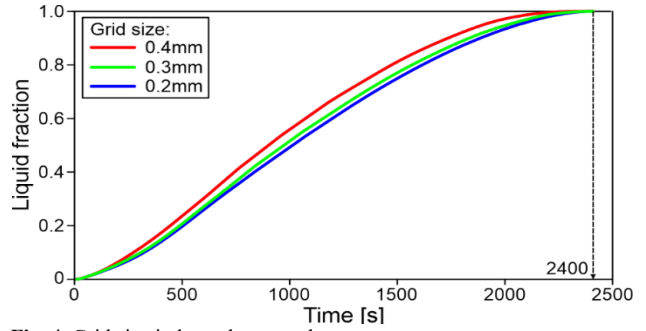


Fig. 4. Grid size independence study.

The Semi-Implicit Method for Pressure Linked Equations – Consistent (SIMPLEC) algorithm was selected to solve the pressure-velocity coupling equations. SIMPLE uses a relationship between velocity and pressure corrections to enforce mass conservation and to obtain the pressure field. Second order upwind schemes were set for the spatial discretization of the governing equations for pressure, momentum and energy transport. The absolute criteria for the solver convergence at each step iteration for every conserved variable was set equal to $1e^{-6}$.

3. Results and Discussion

3.1. Heat Transfer Enhancement

Fig. 5 presents the liquid fraction evolution for the finned and finless setups. The first conclusion drawn from the diagram of Fig. 5 is that the most efficient configuration is the one with the annular fins since the liquid fraction of the phase change material reaches 1 earlier, in 2400s, than in the other cases. The second more efficient model is the one with the straight fins. In this case liquid fraction becomes 1 after 2700s. The least efficient is the finless setup where liquid fraction progresses very slow and reaches 47% after 2700s. At the point that liquid fraction becomes 1 for the case with the

annular fins, the corresponding value for the model with the straight fins is 0.962 and for the finless setup is only 0.423. Also, considering the fact that liquid fraction reaches 1 for the finless case after 6240s, it is easy to conclude that the finned setups shortened the PCM melting time by 61.5% for the annular fin geometry and by 56.7% for the straight fin geometry. The comparison between the two finned configurations reveals that the use of annular fins causes a decrement of the PCM melting time of about 11.1%. Another interesting observation is the way that the liquid fraction progresses for the two finned models. Although at the first 1000s the phase change material found in the straight finned setup seems to heat up faster, liquid fraction for the annular finned case progresses faster since simulation time reaches 1074s and beyond.

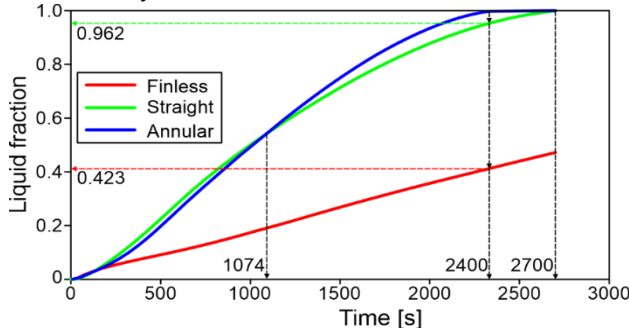


Fig. 5. Liquid fraction versus time for modelled configurations.

Figs. 6 and 7 illustrate the developed temperature fields as well as the liquid fraction of the PCM, on a section shown in the top part of Fig. 6, for two different simulation times. The tube, fins and the shell are not shown as the focus is on the PCM. For every configuration two images are presented. The top one presents the temperature gradient and the bottom one the liquid fraction of the same section.

The first observation from Figs 6 and 7 is that the temperature is higher at the right side of the PCM because water inlet is located at this side in all configurations. Regarding the melting of the PCM, initially a thin layer of PCM in direct contact with the metallic surfaces is heated and change face due to heat conduction. As it is depicted from Fig. 5, liquid fraction increase is more intense after about 200 s. That behavior is attributed to higher thermal resistance of the initial melted PCM, thus limiting heat transfer during the first simulation steps. As the phenomenon progresses, liquid region expands more rapidly due to natural convection driven by the liquid PCM movement which in turn is caused by density differences and gravity. The liquid fraction images of Figs. 6 and 7 reveal that liquid-solid interface moves to areas away from metallic surfaces, proving that the heat transfer mechanism at this stage is driven by natural convection. After most of the PCM has melt, the liquid-solid interface is reduced and thus the role of natural convection on heat transfer is limited.

The comparison of the temperature and liquid fraction gradients between the different configurations for the same simulation time, depicts the effectiveness of the finned setups against the finless considering heat transfer. At 520s, the temperature of the PCM in the finless setup is higher at the region in contact with the tube than in the finned models. That observation changes as we move away from the tube. The PCM temperature of the finned setups is now higher. At 1520s there is a large PCM region in the finless model with a liquid fraction less than 0.1 (Fig. 7), which is not present at the other two setups. Also, the PCM temperature of the exchanger with the annular fins is higher than the PCM in the configuration

with the straight fins. Additionally, multiple liquid – solid interfaces are formed in the PCM of the annular model, as in the case with the straight fins, but the total surface is larger, which explains the faster melting of the PCM in the annular model.

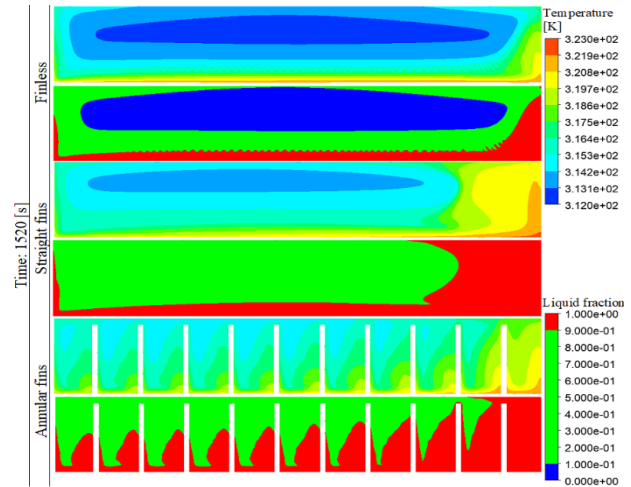


Fig. 6. Temperature and liquid fraction gradients after 540 [s].

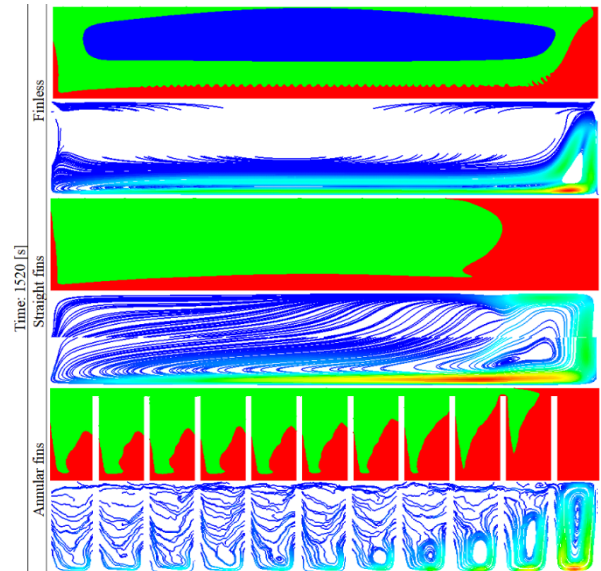


Fig. 7. Temperature and liquid fraction gradients at time 1520 [s].

3.2. Heat Transfer Mechanisms

As mentioned earlier, during the initial simulation steps conduction is the primary heat transfer mechanism and when solid PCM changes phase to liquid, then natural convection becomes the lead heat transfer mechanism. Natural convection involves the interaction of at least a fluid and a solid, where the fluid's velocity is non zero with respect to the solid. In order to get a deeper insight on the convection heat transfer mechanism for the three exchangers, it is necessary to know the velocity profile of the liquid PCM. Fig. 8 illustrates the computed velocity streamlines of the liquid PCM for the same simulation time for the three setups.

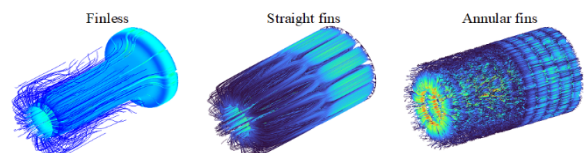


Fig. 8. Velocity streamlines of the liquid PCM for the three heat exchangers at time 2100 [s].

There is an obvious differentiation of the flow pattern between the first two configurations (finless and straight fins) with the one having the annular fins. In the first case the flow is axial whereas in the second case the flow is radial. In addition, the larger number of streamlines of the liquid PCM in the heat exchanger with the straight fins in comparison to the finless setup corresponds to the difference of the liquid fraction of the two models, again for the same simulation timestep. There is not radial fluid movement for the first two models, as there is no axial fluid travel for the third setup.

The density variances of the melted PCM as well as the temperature differences of the various parts of the heat exchangers (hot parts: tube and fins, cold parts: shell) force the liquid PCM to move from the hot surfaces to the cold ones, in a circular manner. This behavior is clearly illustrated in Fig. 9, in which the liquid fraction gradient image is followed by the velocity streamlines one, for the three heat exchangers. Heat travels from the hot surfaces to the moving fluid and lastly to the solid PCM. In the fined exchangers multiple compartments are formed between the tube, the fins and the shell. Although the PCM volume is almost the same for the compartments of the two fined models, the way that liquid PCM travels has a positive effect in the case with the annular fins, as it seems that the total surface of the liquid-solid interface is becomes larger for this case after 1074s.

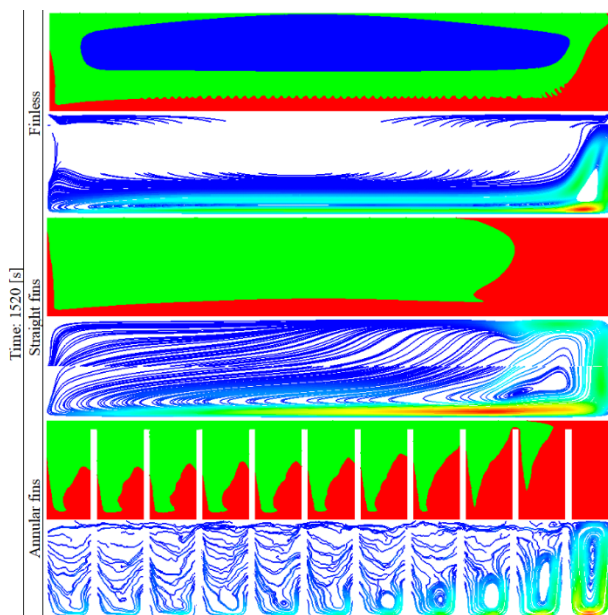


Fig. 9. Liquid fraction and velocity streamlines at time 1520 [s].

4. Conclusion

Computational Fluid Dynamics (CFD) was extensively used in this study to determine the effectiveness of two different, in terms of geometric orientation, heat transfer enhancement methods. In order to describe the involved physics as accurate as possible, the solidification and melting model as well as temperature depended material properties, of the RT42 paraffin, were used. The major findings of this work are the following:

1. Both proposed methods, adding straight or annular fins, proved to be an effective solution for the enhancement of the heat transfer during the melting process of a PCM.
2. Between the two proposed methods, the use of straight fins reduced PCM melting time by 56.7%. On the other hand, the model with the annular fins reduced PCM melting time by 61.5%.
3. During melting the liquid PCM travels from the hot surfaces to the cold ones. Because of this movement natural convection is the lead heat transfer mechanism.
4. Annular fins seem to be more effective than straight ones. This can be attributed to the total liquid-solid interface being larger than the corresponding one of the model with the straight fins.

Acknowledgments

The work was implemented in the framework of the project "A Thermal Storage Pilot Plant using Bio-based Phase Changing Materials" T1EAK-00947, co-financed by the: Greek State, EU, in the framework of the Operational Program "Competitiveness, Entrepreneurship & Innovation" (EPAnEK) of the NSRF 2014–2020, "RESEARCH - CREATE - INNOVATE".

This is an Open Access article distributed under the terms of the Creative Commons Attribution License.



References

1. Saniuk, S.; Grabowska, S.; Gajdzik, B. Personalization of Products in the Industry 4.0 Concept and Its Impact on Achieving a Higher Level of Sustainable Consumption. *Energies*, 13, 2020, pp. 5895.
2. B. Mohammad Olfat, F. Talati. The effects of fins number and bypassed energy fraction on the solidification process of a phase change material, *Journal of Storage Mater.*, 42, 2021, pp. 102957.
3. B. Fekadu, M. Assay. Enhancement of phase change materials melting performance in a rectangular enclosure under different inclination angle of fins Case Study. *Thermal Engineering*, 25, 2021, pp. 100968.
4. X. Yang, S. Feng, Q. Zhang, Y. Chai, L. Jin, T.J. Lu, The role of porous metal foam on the unidirectional solidification of saturating fluid for cold storage, *Applied Energy*, 194, 2017, pp. 508-521.
5. Z. Zhang, X. He, Three-dimensional numerical study on solid-liquid phase change within open-celled aluminum foam with porosity gradient, *Applied Thermal Engineering*, 113, 2017, pp. 298-308.
6. J. Woodfield, M. Alvarez, B. Gómez-Vargas, R. Ruiz-Baier, Stability and finite element approximation of phase change models for natural convection in porous media, *Journal of Computational and Applied Mathematics*, 360 2019, pp. 117–137.
7. X. Liu, T. Cai, S. Jiang, Z. Jiang, F. He, Y. Li, R. He, K. Zhang, W. Yang, Experimental study and numerical simulation of heat transfer behavior based on silicone rubber/paraffin @SiO₂ shape-stabilized phase change material, *Journal of Energy Storage*, 44, 2021, pp. 103431.
8. J. Wang, H.Sh. Majdi, H.A. Dhahad, T.A. Nofal, A.S. Alghawli, P. Xu, Simulation of heat release from phase change material with insert of fins and addition of nano-powders, *Journal of Energy Storage*, 52, 2022, pp. 104680.
9. Y. Gao, J. Jin, T. Xiao, M. Liu, S. Liu, R. Liu, J. Pan, G. Qian, X. Liu, Study of temperature-adjustment asphalt mixtures based on silica-based composite phase change material and its simulation, *Construction and Building Materials*, 342, 2022, pp. 127871.

10. G. Fang, P. Sun, M. Zhao, W. Zhang, Experimental and numerical simulation of paraffin-based ternary composite phase change material used in solar energy system, *Applied Thermal Engineering*, 214, 2022, pp. 118618.
11. S. Al-Musaedi, Z. Asadi, D.D. Ganji, M. Javidan, Simulation of melting and solidification processes of organic phase change materials used in storing heat energy in multi-layers heat exchanger, *Journal of Energy Storage*, 50, 2022, pp. 104687.
12. Diani, C. Nonino, L. Rossetto, Melting of phase change materials inside periodic cellular structures fabricated by additive manufacturing: Experimental results and numerical simulations, *Applied Thermal Engineering*, 215, 2022, pp. 118969.
13. W. Cui, T. Si, X. Li, X. Li, L. Lu, T. Ma, Q. Wang, Heat transfer analysis of phase change material composited with metal foam-fin hybrid structure in inclination container by numerical simulation and artificial neural network, *Energy Reports*, 8, 2022, pp. 10203–10218.
14. M. Gharebaghi, I. Sezai, Enhancement of Heat Transfer in Latent Heat Storage Modules with Internal Fins, *Numerical Heat Transfer, Part A: Applications*, 53, 2007, pp.749–765.
15. M. K. Rathod, J. Banerjee, Thermal Performance Enhancement of Shell and Tube Latent Heat Storage Unit Using Longitudinal Fins, *Applied Thermal Engineering*, 75, 2015, pp. 1084–1092.
16. G. Wei, G. Wang, Y. Yang, C. Xu, X. Du, Pore-scale numerical simulation of melting process of PCMs in foam metals, Paper presented at the *International Heat Transfer Conference*, 2018, pp. 4979-4984.
17. ANSYS fluent software package: user's manual, 18.0, 2017.